Thermodynamic Investigation of the Ni-Rich Side of the Ni−P System

Simona Delsante,[†] Clemens Schmetterer,[‡] Herbert Ipser,[‡] and Gabriella Borzone*[,†]

Department of Chemistry and Industrial Chemistry, University of Genoa, INSTM UdR Genoa, Via Dodecaneso 31, I-16146 Genoa, Italy, and Department of Inorganic Chemistry/Materials Chemistry, University of Vienna, Währingerstr. 42, A-1090 Wien, Austria

Ni(P) is used in electronics as a protective layer during the soldering process. New thermodynamic information on Ni−P alloys has been obtained in the Ni-rich part (up to the molar fraction $x_P = 0.40$) by using a high-temperature direct drop calorimeter. The experimental trend of $\Delta_f H°$ [kJ·(mol of atoms)$^{-1}$] of the Ni−P alloys versus composition (x_P) has been plotted and the following standard enthalpy of formation [$\Delta_f H° \pm 2$ kJ·(mol of atoms)$^{-1}$] values interpolated for the Ni-rich phases: −48.0 (Ni_3P), −55.0 (Ni_5P_2), −56.0 ($Ni_{12}P_5$), and −61.0 (NiP_2). Our results have been compared with those reported in the literature and discussed.

Introduction

General Remarks. The transition metal phosphides are an interesting class of compounds that combine the physical properties of ceramic materials, such as hardness and strength, with the transport properties of metals, such as thermal and electrical conductivity. They can be prepared easily from inexpensive phosphate precursors by a reduction in hydrogen.[1] The transition metal phosphides have been widely studied because of their possible applications in many different fields of technological interest. They are a group of stable, sulfur-resistant, metallic compounds that have been found to have exceptional properties that can be applied as catalysts for hydrodesulfurization (HDS) and hydrodenitrogenation (HDN) processes[2] to fulfill the increasingly stringent environmental regulations concerning the removal of sulfur, a very important problem in the refining industry.[3,4] Various work has shown that MoP,[5,6] WP,[7] Ni_2P, and Co_2P[8] are highly active for HDS and HDN of petroleum stocks.

The Ni−P system is also one of the most extensively studied glasses, and its behavior is representative of the metal−nonmetal class of glasses. Ni−P alloy films obtained by electroless plating have been widely used for corrosion resistance and nonmagnetic coatings owing to their superior properties.[9,10] In microelectronics, solder joint integrity and material selection for various metallization layers are critical issues. Electroless Ni−P is widely used for under bump metallization (UBM) of flip chip and surface finish layers in microelectronics packaging because of its excellent solderability, corrosion resistance, uniformity, and also as good diffusion barrier. For example, the electroless plating technique is employed in the electronics industry to deposit a protective layer of Ni(P) on the Cu metallization for ball grid array (BGA) assemblies in a phosphorus-containing-bath; the Ni(P) layers can be created with a x_P content of even more than 0.20. During the soldering process, this Ni(P) layer reacts with the solder to form a layer of intermetallic phases (e.g., Ni_3P, Ni_2PSn).[11−13]

* Corresponding author. Phone: +39 010 3536153. Fax: +39 010 3625051. E-mail address: gabriella.borzone@unige.it.
[†] University of Genoa.
[‡] University of Vienna.

Knowledge of the stability of the intermetallic phases and their thermodynamic properties are, therefore, very important tools for thermodynamic description of the binary alloys to extrapolate more complex systems (e.g., Ni−Sn−P). At the same time, coherent and reliable data obtained by using different experimental techniques in various laboratories form the basis for an accurate collection of the set of data to be used in CALPHAD modeling and can provide an updated thermodynamic database for lead-free solder materials and substrates.

State of the Art Research. Lee and Nash[14] summarized the crystal structures and lattice constants of Ni−P intermediate phases, the existence of metastable phases, and thermodynamic information, as well as assessing the phase diagram of the Ni−P system by compiling a large amount of information published in the literature since 1908. In the Ni-rich part of the diagram (up to $x_P \sim 0.40$) four intermetallic phases exist: Ni_3P, Ni_5P_2 (low temperature, LT, and high temperature, HT, forms), $Ni_{12}P_5$ (LT and HT forms), and Ni_2P.

On the basis of these data Shim et al.[15] performed a thermodynamic evaluation of the Ni−P binary system with the CALPHAD method and described the glass-forming ability of this system by using a simple kinetic model.

The thermodynamic properties of phosphorus and solid binary phosphides have been critically reviewed by Schlesinger.[16]

A very recent new version of the Ni−P phase diagram was established by Schmetterer et al.[17] based on X-ray diffraction (XRD), electron probe microanalysis (EPMA), and differential thermal analysis (DTA) measurements. They found some significant differences from the previous versions; concerning the Ni-rich part, they confirmed the presence of the Ni_3P, Ni_5P_2 LT, $Ni_{12}P_5$ LT, and Ni_2P phases in good agreement with the compositions previously reported in the literature. The Ni_3P, Ni_5P_2 LT, and $Ni_{12}P_5$ LT phases have been confirmed to be line compounds, while for Ni_2P they proposed a range of solubility and a congruent formation at 1378 K. The existence of the Ni_5P_2 HT and $Ni_{12}P_5$ HT phases was confirmed with a homogeneity range and with a peritectic and congruent formation, respectively; the region of the two HT phases appears to be quite different from that previously reported in the literature.

Several researchers experimentally investigated the thermodynamic properties of the Ni−P system.

10.1021/je100166z
Published on Web 07/12/2010

Table 1. Literature Data: Enthalpy of Formation in Ni−P System [kJ·(mol of atoms)$^{-1}$]

		T_{ref} (K)/Experimental Technique/Reference								
					T = 298/Knudsen cell effusion					
phase	mole fraction P (x_P)	T = 300 H.T. calorimetry (this work)	T = 903 H.T. calorimetry[18]	T = 298 H.T. calorimetry[19]	20	22	21	calculated CALPHAD method[15]	calculated ab initio[24]	Miedema[25]
Ni_3P	0.250	−48 ± 2	−50.6		−49 ± 4	−49.5 ± 1.2	−51.7 ± 3	−50.4	−29	−45
Ni_5P_2	0.286	−55 ± 2	−57.3	−52.1 ± 2.0[a]	−55 ± 4	−54.2 ± 1.3		−55.4		−50
$Ni_{12}P_5$	0.294	−56 ± 2			−56 ± 4	−54.8 ± 1.3		−56.7	−7.9	−51
Ni_2P	0.333	−61 ± 2	−55.7		−57 ± 4	−55.7 ± 1.3			−22.3	−56
Ni_5P_4	0.444		−51.9		−53 ± 4					−62
NiP_2	0.667		−41.7		−45 ± 4					−42
NiP_3	0.750		−34.5		−38 ± 4					−28

[a] In ref 19 is reported an overall composition of $Ni_{2.55}P$ (x_P = ~0.282). H.T. = high temperature.

Table 2. Summary of Calorimetric Results for the Reaction yNi(s) + xP(s) → Ni_yP_x(s)[a]

Id.	composition/mol fraction P	working T (± 2 °C)	$\Delta_fH°$ ± 2 kJ·(mol of atoms)$^{-1}$	comments on SEM/EPMA analysis
1	0.180	681	−39.0	10 % of primary crystals of Ni and 90 % of eutectic Ni_3P−Ni, see Figure 1
2	0.220	654	−41.0	80 % of primary crystals of Ni_3P and 20 % of eutectic Ni_3P−Ni, see Figure 2
3	0.230	778	−41.5[b]	not uniform sample
4	0.250	696	−44.3[c]	80 % of Ni_3P crystals, 10 % of eutectic Ni_3P−Ni, and 10 % of Ni_5P_2 phase
5	0.250	733	−46.0	90 % of Ni_3P crystals, around 10 % of eutectic Ni_3P−Ni, presence of Ni_5P_2, phase
6	0.250	655	−47.0	90 % of Ni_3P crystals, around 10 % eutectic Ni_3P−Ni, presence of Ni_5P_2, phase.
7	0.270	778	−47.5	almost one-phase sample Ni_5P_2 and few crystals of $Ni_{12}P_5$
8	0.280	789	−49.5	almost one-phase sample Ni_5P_2, presence of few crystals of $Ni_{12}P_5$ phase
9	0.286	746	−43.9[b]	incomplete reaction
10	0.290	780	−54.0	90 % of Ni_5P_2 phase and 10 % $Ni_{12}P_5$ phase
11	0.310	792	−59.0	90 % of $Ni_{12}P_5$ phase and 10 % of Ni_2P phase
12	0.340	789	−60.0	95 % of Ni_2P phase and 5 % of Ni_5P_4 phase, see Figure 3
13	0.370	778	−48.0[b]	90 % Ni_2P and 10 % Ni_5P_4
14	0.400	778	−52.6	80 % Ni_2P and 20 % Ni_5P_4

[a] The reference states are fcc-Ni and red P. [b] Rejected value. [c] Considered as lower limited value.

Data concerning the enthalpy of formation of the Ni−P intermetallic phases are reported in Table 1 together with the experimental technique used, the reference temperature, and the results obtained in the investigation. Only Weibke and Schrag[18] and Boone and Kleppa[19] performed direct measurements. Weibke and Schrag measured the enthalpies of formation of Ni−P alloys using high-temperature calorimetry; Boone and Kleppa[19] used a high-temperature calorimeter dropping the pellets sealed into a quartz container into an adiabatic shield calorimeter operating around 903 K. In both papers no information was given about the control of the composition of the synthesized alloys, the phases formed, and their composition.

Myers and Conti[20] evaluated the enthalpies of formation of Ni−P alloys at 298 K using the Knudsen cell effusion method and obtained results in good agreement with those by refs 18 and 19 within the margin of error. With the same technique Viksman and Gordienko[21] and, more recently, Zaitsev et al.[22] performed new measurements. Michimoto et al.[23] performed equilibrium experiments between molten lead and six combinations of two adjacent nickel phosphides (Ni−Ni_3P, Ni_3P−Ni_5P_2, Ni_5P_2−$Ni_{12}P_5$, $Ni_{12}P_5$−Ni_2P, Ni_2P−Ni_5P_4, and Ni_5P_4−NiP_2) in the temperature range (973 to 1123) K. The activity coefficient of nickel in molten lead was evaluated by assuming that Henry's law was applicable to the activity of nickel and by neglecting the interaction between nickel and phosphorus in molten lead. The standard Gibbs energies of various reactions were evaluated, but no enthalpy data were reported.

Calculated values of the enthalpies of formation obtained by the CALPHAD method,[15] by ab initio calculations,[24] and with the Miedema model[25] are also reported in Table 1. The experimental data determined in this work are also included for comparison.

The purpose of this work is the experimental investigation of the enthalpy of formation of the Ni−P alloys by using a high-temperature direct drop calorimeter. This work is carried out in the framework of the European COST Action MP0602 on Advanced Solder Materials for High Temperature Application (HISOLD).

Experimental Section

Ni−P calorimetric mechanical mixtures were prepared in the Department of Inorganic Chemistry/Materials Chemistry of Vienna University by mixing proper amounts of Ni (99.995 %, Koch Light Laboratories, UK) and P (red P lump, 99.999+ %, Alfa Aesar, Germany) powders in a composition range of x_P from 0.16 to 0.40. The powders were thoroughly mixed and pressed into pellets weighing about 0.4 g. In the Genoa laboratory, the pellets for calorimetric measurements were put inside a small alumina crucible enclosed in a tight-sealed Ta crucible. The use of sealed Ta crucibles prevents any phosphorus loss, thus avoiding any damage to the calorimeter and changes in sample composition.

All of these technical solutions have been employed to overcome different experimental difficulties due to the intrinsic factors of the system such as a large difference in melting point between Ni and P, high vapor pressure of P, and reactivity of P with Ta crucibles for which the use of an alumina crucible was necessary.

Calorimetric Measurements. Calorimetric measurements were performed with a laboratory-built high-temperature drop

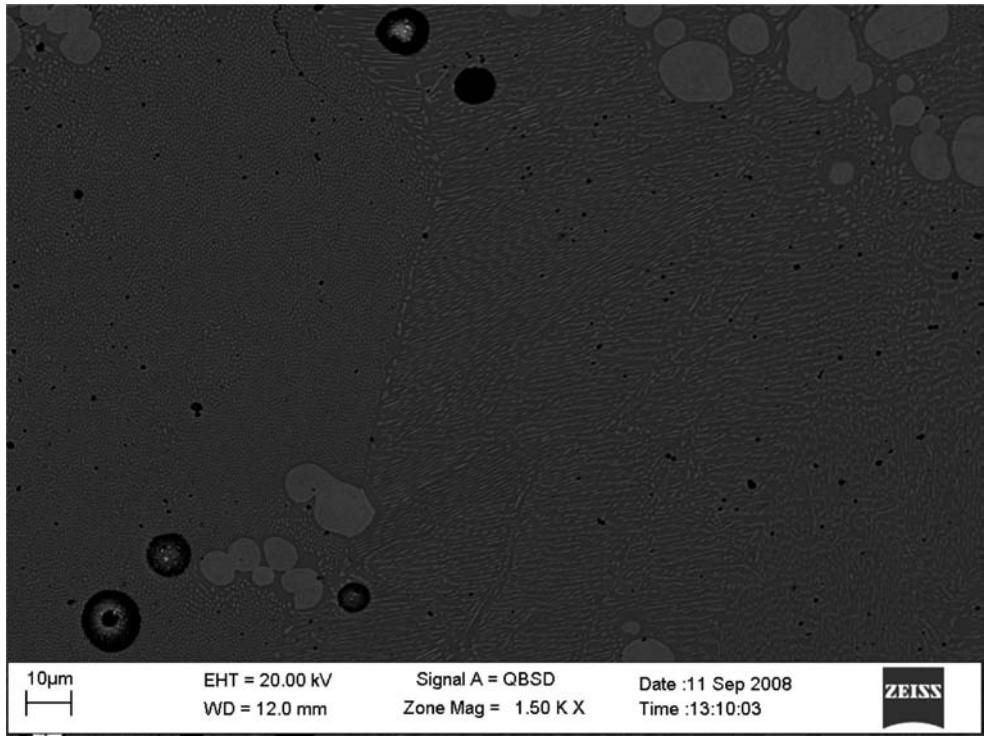

Figure 1. SEM micrograph appearance (BSE signal), after calorimetric measurement, of the $Ni_{0.82}P_{0.18}$ specimen (#1, Table 2); primary white crystals of Ni surrounded by the fine eutectic Ni_3P-Ni. The black holes reveal the porosity of the surface after synthesis.

calorimeter, a detailed description of which is reported elsewhere.[26,27] Following the composition of the alloys, the working calorimeter temperature was set at values included between (923 and 1073) K. Each calorimetric measurement is divided into two runs: a "reaction run" and a "reference run"; an exhaustive description of the procedure is given in ref 28. To perform a measurement, after thermal equilibration, the sample is dropped from an overstanding thermostat (at $T = T_0 = 300$ K) into the calorimeter. This is referred to as the reaction run. The heat effect is evaluated by a series of calibration runs performed by dropping specimens of known heat content (typically pieces of pure silver weighing (1.0 to 1.5) g). In the following we report the reaction occurring and the equations used to determine the measured heat.

In the reaction run the heat effect Q_1 is due to the reaction:

$$y\mathrm{Ni}(\mathrm{cr},T_c) + x\mathrm{P}(\mathrm{cr},T_c) \rightarrow \mathrm{Ni}_y\mathrm{P}_x(\mathrm{cr},T_c)$$

at T_c working calorimetric temperature and also due to the increment of enthalpy of Ni and P and of the crucible.

Therefore, Q_1 for 1 mol of alloy Ni_yP_x is

$$Q_1 = y(H^\circ_{T_c} - H^\circ_{T_0})(\mathrm{Ni,cr}) + x(H^\circ_{T_c} - H^\circ_{T_0})(\mathrm{P,cr}) + (H^\circ_{T_c} - H^\circ_{T_0})(\mathrm{cruc}) + \Delta_f H^\circ(\mathrm{Ni}_y\mathrm{P}_x,\mathrm{cr},T_c)$$

In the reference run, the heat effect Q_2 is due to the enthalpy increments of the compound and of the crucible

$$Q_2 = (H^\circ_{T_c} - H^\circ_{T_0})(\mathrm{Ni}_y\mathrm{P}_x,\mathrm{cr}) + (H^\circ_{T_c} - H^\circ_{T_0})(\mathrm{cruc})$$

By taking the difference, $(Q_1 - Q_2)$, the crucible effects are canceled out. The result is the $\Delta_f H^\circ(Ni_yP_x, \mathrm{cr}, T_c)$, corrected for the difference in the heat contents of metals and compound, that is, the $\Delta_f H^\circ(Ni_yP_x, \mathrm{cr}, T_0)$ at T_0

$$Q_1 - Q_2 = \Delta_f H^\circ(\mathrm{Ni}_y\mathrm{P}_x,\mathrm{cr},T_0)$$

The measurement errors are estimated to be $\pm$ (0.3 to 0.5) kJ·(mol of atoms)$^{-1}$ in any run. The accuracy of calorimetric measurements is related to the actual processes occurring in the calorimeter. The sensitivity of the calorimeter was obtained by dropping under different conditions (mass, temperature) several samples of known heat content as a function of the total mass accumulated in the measuring cell. Besides, further tests carried out by dropping Ag samples of different masses into the calorimeter at 973 K showed that the sensitivity is independent of the size of heat effect in the energy range between (50 and 1000) J. To make an overall evaluation, the completeness of the synthesis reaction, attainment of the equilibrium state, presence/absence of side reactions, and so forth should be considered. We have also checked that no reaction occurred with Ta crucibles during the calorimetric synthesis of the Ni−P samples. In this study, an error associated with the measurement of standard enthalpy of formation ($\Delta_f H^\circ$) is estimated to be $\pm$ 2 kJ·(mol of atoms)$^{-1}$. The composition of the sample and the related working temperature of the calorimeter were carefully selected on the basis of the information available on the phase diagram to have fast synthesis reactions (see Table 2). Moreover, after the measurements, composition and state of the samples were examined by means of microscopic analysis (optical and electron probe microanalysis).

Characterizations. The microstructure of the alloys was first observed by light optical microscopy by a Leica DM4000 M microscope equipped with a Leica DFC camera and X-Plus Alexasoft software. Subsequently, a thorough investigation of each sample was completed using an electron scanning micro-

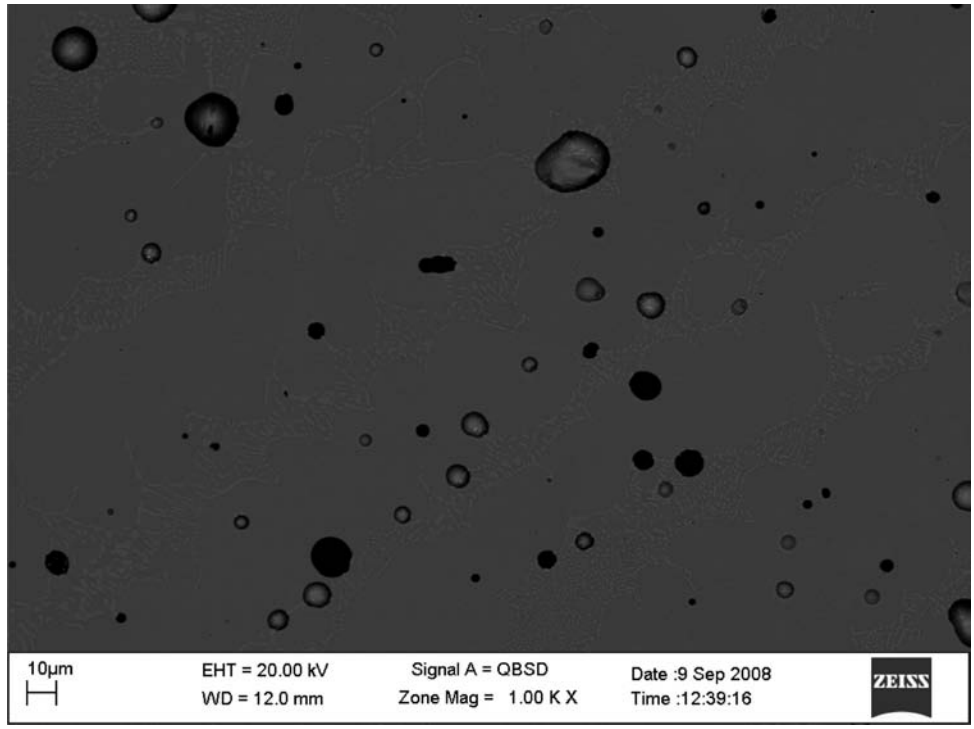

Figure 2. SEM micrograph appearance (BSE signal), of the $Ni_{0.78}P_{0.22}$ specimen (#2 in Table 2) after calorimetric measurement: primary gray crystal of Ni_3P surrounded by the eutectic Ni_3P-Ni. The black holes reveal the porosity of the surface after synthesis.

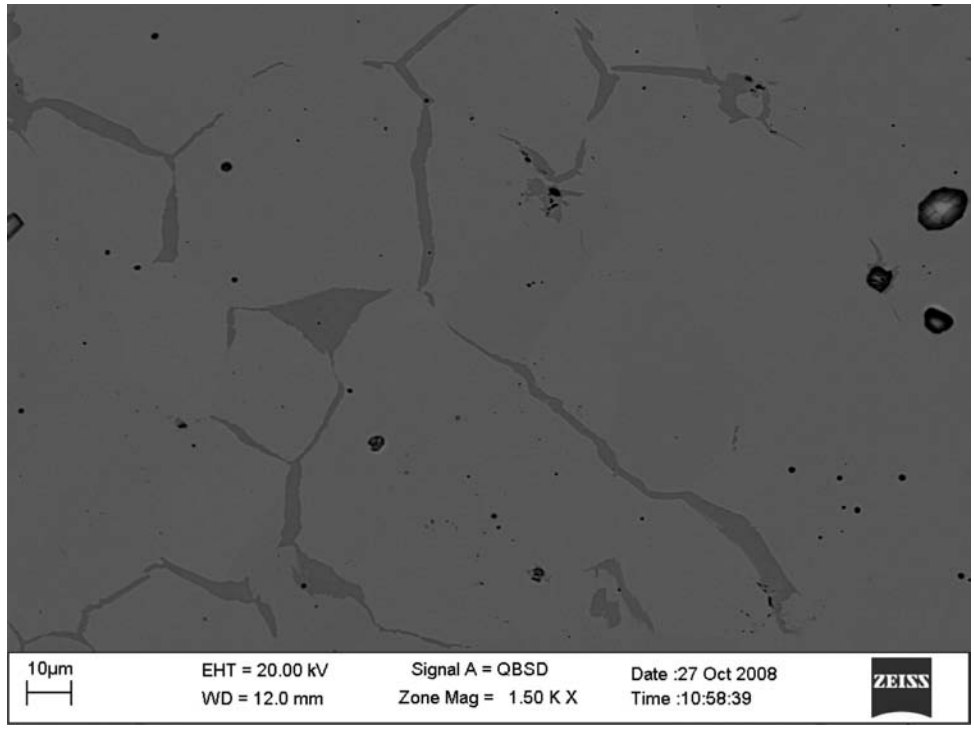

Figure 3. SEM micrograph appearance (BSE signal), after calorimetric measurement, of the $Ni_{0.66}P_{0.34}$ specimen (#12 in Table 2): Ni_2P prevalent gray phase and Ni_5P_4 dark-gray phase.

scope (Zeiss-EVO 40). The compositional contrast between the different phases was obtained by a backscattered electron (BSE) detector, and quantitative data were collected at 20 kV on a Link System Ltd. Instrument, equipped with an energy dispersive spectrometry (EDS) detector. A counting time of 100 s and a ZAF correction program were used. Certified pure elements were used as reference standards, while cobalt was adopted for calibration purposes. The software package Inca Energy (Oxford Instruments, Analytical Ltd., Bucks, U.K.) was employed to process X-ray spectra.

Results and Discussion

After the calorimetric measurements the synthesized samples are shiny, hard, and quite brittle. To check whether the equilibrium state has been reached and check for side reactions,

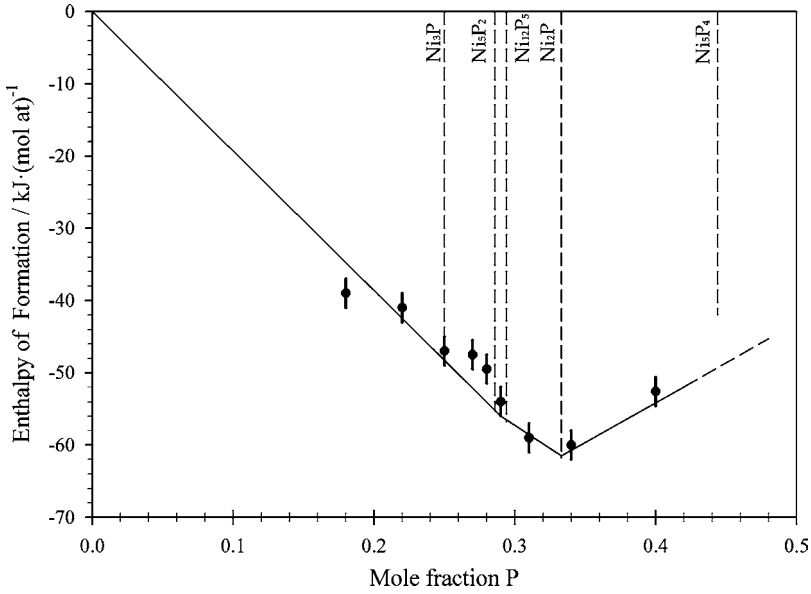

Figure 4. Experimental trend of $\Delta_f H°$ [kJ·(mol of atoms)$^{-1}$] vs composition of the Ni−P alloys (see Table 2).

the different samples prepared in the calorimeter were characterized by scanning electron microscopy (SEM) and EDS analysis.

The appearance of the SEM micrograph of the specimen $Ni_{0.82}P_{0.18}$ composition (#1 in Table 2) using the BSE signal is given in Figure 1: the primary white crystals of Ni are surrounded by the fine eutectic Ni_3P/Ni, and the black holes reveal the porosity of the surface. Figure 2 shows the SEM micrograph (BSE signal), of the specimen $Ni_{0.78}P_{0.22}$ (#2 in Table 2): the primary gray crystals of Ni_3P are surrounded by the eutectic Ni_3P/Ni, and the porosity of the surface is easily recognizable. The SEM micrograph (BSE signal) of the $Ni_{0.66}P_{0.34}$ calorimetric sample (#12 in Table 2) given in Figure 3 shows a prevalent Ni_2P gray phase surrounded by the Ni_5P_4 dark-gray phase at the grain boundaries.

From the EDS analysis on the calorimetric samples, we confirm the sequence of the intermetallic phases reported in the literature together with their atomic composition. However, for the eutectic Ni/Ni_3P a global composition of about $x_P = 0.20$ was systematically detected as well as $x_P = 0.26$ composition for the Ni_3P phase, slightly different from the composition reported in the literature which are $x_P = 0.19$ for the global composition of the eutectic Ni/Ni_3P and $x_P = 0.25$ for the Ni_3P phase.

The data corresponding to samples which reached the equilibrium state were used to determine the trend of $\Delta_f H°$ versus composition (see Figure 4) and to evaluate the most reliable values of the standard enthalpies of formation for the different compounds. The enthalpies of formation of the investigated Ni−P alloys together with the experimental calorimetric temperature and SEM-EDS results are reported in Table 2. The standard enthalpy of formation interpolated values [$\Delta_f H°$ ± 2 kJ·(mol of atoms)$^{-1}$] are summarized in Table 1 and are the following: −48.0 (Ni_3P), −55.0 (Ni_5P_2), −56.0 ($Ni_{12}P_5$), and −61.0 (NiP_2).

As can be noticed in Table 1, our results are in very good agreement with the data by Myers and Conti obtained using the Knudsen effusion method[19] and agree fairly well with the other values.

Conclusions

The high thermodynamic stability of the Ni−P alloys has been confirmed, and a highly exothermic behavior was observed around $x_P = 0.29$ composition (close to Ni_5P_2 and $Ni_{12}P_5$) and the Ni_2P phase. This behavior may be correlated to strong metal−P bonds present in these compounds as observed by Harris.[29] He carried out a comprehensive study of the electronic structure and bonding on MP (M = Mo, W, Co) and M_2P (M = Co, Ni), and the results show that there are strong metal−P bonds in both Co_2P and Ni_2P, while there is no metal−metal bonding in either material, since both the metal−metal bonding and the antibonding bands are occupied.

The highest stability of the Ni_2P phase was also predicted by Ren et al.[30] on the basis of their systematic study of the structure, bonding, and relative thermodynamic stability of the crystalline nickel phosphides, for which they carried out calculations by using density functional theory.

Literature Cited

(1) Clark, P.; Li, W.; Oyama, S. T. Synthesis and Activity of a New Catalyst for Hydroprocessing: Tungsten Phosphide. *J. Catal.* **2001**, *200*, 140–147.
(2) Oyama, S. T. Novel catalysts for advanced hydroprocessing: transition metal phosphides. *J. Catal.* **2003**, *216*, 343–352.
(3) Greening, P. European Vehicle Emission Legislation−Present and Future. *Top. Catal.* **2001**, *16−17* (1−4), 5–13.
(4) Bertelsen, B. I. Future US Motor Vehicle Emission Standards and the Role of Advanced Emission Control Technology in Meeting Those Standards. *Top. Catal.* **2001**, *16/17*, 15–22.
(5) Stinner, C.; Prins, R.; Weber, Th. Formation, Structure, and HDN Activity of Unsupported Molybdenum Phosphide. *J. Catal.* **2000**, *191*, 438–444.
(6) Stinner, C.; Prins, R.; Weber, Th. Binary and Ternary Transition-Metal Phosphides as HDN Catalysts. *J. Catal.* **2001**, *202*, 187.
(7) Oyama, S. T.; Clark, P.; Wang, X.; Shido, T.; Iwasawa, Y.; Hayashi, S.; Ramallo-Lòpez, J. M.; Requejo, F. G. Structural Characterization of Tungsten Phosphide (WP) Hydrotreating Catalysts by X-ray Absorption Spectroscopy and Nuclear Magnetic Resonance Spectroscopy. *J. Phys. Chem. B* **2002**, *106*, 1913–1920.
(8) Wang, X.; Clark, P.; Oyama, S. T. Synthesis, Characterization, and Hydrotreating Activity of Several Iron Group Transition Metal Phosphides. *J. Catal.* **2002**, *208*, 321–331.
(9) Park, S. H.; Lee, D. N. A study on the microstructure and phase transformation of electroless nickel deposits. *J. Mater. Sci.* **1988**, *23*, 1643–1654.
(10) Hur, K. H.; Jeong, J. J.; Lee, D. N. Microstructures and crystallization of electroless Ni-P deposits. *J. Mater. Sci.* **1990**, *25*, 2573–2584.
(11) He, M.; Chen, Z.; Qi, G.; Wong, C. C.; Mhaisalkar, S. G. Effect of post-reflow cooling rate on intermetallic compound formation between Sn-3.5 Ag solder and Ni-P under bump metallization. *Thin Solid Films* **2004**, *462−463*, 363–369.

(12) Yoon, J. W.; Kim, S. W.; Jung, S. B. Effect of reflow time on interfacial reaction and shear strength of Sn-0.7Cu solder/Cu and electroless Ni-P BGA joints. *J. Alloys Compd.* **2004**, *385*, 192–198.
(13) Lin, Y. C.; Shih, T. Y.; Tien, S. K.; Duh, J. G. Morphological and Microstructural Evolution of Phosphorous-Rich Layer in SnAgCu/Ni-P UBM Solder Joint. *J. Electron. Mater.* **2007**, *36*, 1469–1475.
(14) Lee, K. J.; Nash, P. *Phase Diagrams of Binary Nickel Alloys*; Nash, P., Ed.; ASM International: Materials Park, OH, 1991; p 235.
(15) Shim, J. H.; Chung, H. J.; Lee, D. N. Calculation of phase equilibria and evaluation of glass-forming ability of Ni-P alloys. *J. Alloys Compd.* **1999**, *282*, 175–181.
(16) Schlesinger, M. E. The Thermodynamic Properties of Phosphorous and Solid Binary Phosphides. *Chem. Rev.* **2002**, *102*, 4267–4301.
(17) Schmetterer, C.; Vizdal, J.; Ipser, H. A new investigation of the system Ni-P. *Intermetallics* **2009**, *17* (10), 826–834.
(18) Weibke, F.; Schrag, G. Die Bildungswärmen der Niederen Phosphide Einiger Schwermetalle. *Z. Elektrochem. Angew. Phys. Chem.* **1941**, *47* (3), 222–238.
(19) Boone, S.; Kleppa, O. J. Determination of the standard enthalpy of formation of $Ni_{2.55}P$ by high-temperature drop calorimetry. *J. Chem. Thermodyn.* **1991**, *23*, 781.
(20) Myers, C. E.; Conti, T. J. Vaporization behavior, phase equilibria, and thermodynamic stabilities of nickel phosphides. *J. Electrochem. Soc.* **1985**, *132* (2), 454–457.
(21) Viksman, G. Sh.; Gordienko, S. P. High-Temperature Behavior of Nickel Phosphide in Vacuum and Its Thermodynamic Characteristics. *Poroshk. Metall.* **1992**, *12*, 70–72.
(22) Zaitsev, A. I.; Zaitseva, N. E.; Shakhpazov, E. Kh. Thermodynamic Properties of Intermediate Ni-P Phases (26−32.5 at. % P) between 971 and 1440 K. *Inorg. Mater.* **2003**, *39* (5)), 427–432.
(23) Michimoto, T.; Suzuki, N.; Oishi, T. Solubilities of Nickel and Phosphorus in molten lead. *Trans. Inst. Min. Metall., Sect. C* **2008**, *117* (4), 236–239.
(24) Press, M. R.; Khanna, S. N.; Jena, P. Electronic structure, magnetic behavior, and stability of Ni-P. *Phys. Rev. B: Condens. Matter Mater. Phys.* **1987**, *36* (10), 5446–5453.
(25) de Boer, F. R.; Boom, R.; Mattens, W. C. M.; Miedema, A. R.; Niessen, A. K. In *Cohesion in Metals: Transition Metal Alloys*; de Boer, F. R., Pettifor, D. G., Eds.; North-Holland: Amsterdam, 1988; Vol. 1.
(26) Cacciamani, G.; Borzone, G.; Ferro, R. On a simple high temperature direct reaction calorimeter. *J. Alloys Compd.* **1995**, *220*, 106–110.
(27) Borzone, G.; Raggio, R.; Ferro, R. Remarks on the role of thermochemical data in intermetallic crystallochemistry. *J. Alloys Compd.* **2004**, *367*, 89–102.
(28) Ghosh, G.; Delsante, S.; Borzone, G.; Asta, M.; Ferro, R. Phase stability and cohesive properties of Ti-Zn intermetallics: First-principles calculations and experimental results. *Acta Mater.* **2006**, *54*, 4977–4997.
(29) Harris, S. 52nd Annual report on research, Wyoming University, 44045-AC5, 2007, http://www.acsprf-ar.org/2007/REPORTS/P8076.HTM.
(30) Ren, J.; Wang, J. G.; Li, J. F.; Li, Y. W. Density functional theory study on crystal nickel phosphides. *J. Fuel Chem. Technol.* **2007**, *35* (4), 458–464.

Received for review February 16, 2010. Accepted June 12, 2010. This work is a contribution to the European COST Action MP0602 on Advanced Solder Materials for High Temperature Application (HISOLD).

JE100166Z